

# Power flow control with UPFC

Rusejla Sadikovic  
Internal report

## 1 Unified Power Flow Controller (UPFC)

The UPFC can provide simultaneous control of all basic power system parameters ( transmission voltage, impedance and phase angle). The controller can fulfill functions of reactive shunt compensation, series compensation and phase shifting meeting multiple control objectives. From a functional perspective, the objectives are met by applying a boosting transformer injected voltage and a exciting transformer reactive current. The injected voltage is inserted by a series transformer.

Besides transformers, the general structure of UPFC contains also a "back to back" AC to DC voltage source converters operated from a common DC link capacitor, Figure 1. First converter (CONV1) is connected in shunt and the second one (CONV2) in series with the line. The shunt converter is primarily used to provide active power demand of the series converter through a common DC link. Converter 1 can also generate or absorb reactive power, if it is desired, and thereby provide independent shunt reactive compensation for the line. Converter 2 provides the main function of the UPFC by injecting a voltage with controllable magnitude and phase angle in series with the line via an voltage source, Figure 2. The reactance  $x_s$  describes a reactance seen from terminals of the series transformer and is equal to (in p.u. base on system voltage and base power)

$$x_S = x_k r_{max}^2 (S_B / S_S) \quad (1)$$

where  $x_k$  denotes the series transformer reactance,  $r_{max}$  the maximum per unit value of injected voltage magnitude,  $S_B$  the system base power, and  $S_S$  the nominal rating power of the series converter.

The UPFC injection model is derived enabling three parameters to be simultaneously controlled. They are namely the shunt reactive power,  $Q_{conv1}$ , and the magnitude,  $r$ , and the angle,  $\gamma$ , of injected series voltage  $\bar{V}_{se}$ . The

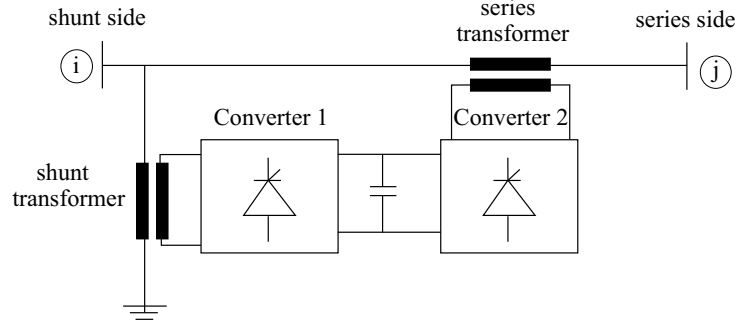


Figure 1: Implementation of the UPFC by back-to-back voltage source converters

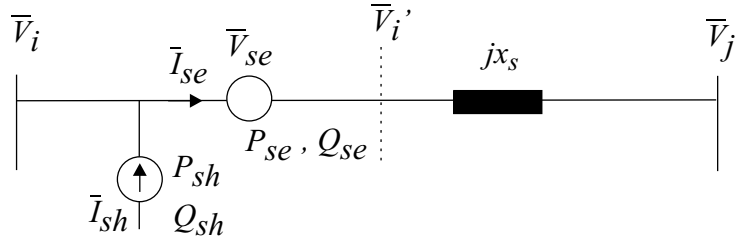


Figure 2: The UPFC electric circuit arrangement

series connected voltage source is modeled by an ideal series voltage  $\bar{V}_{se}$  which is controllable in magnitude and phase, that is,  $\bar{V}_{se} = r\bar{V}_k e^{j\gamma}$  where  $0 \leq r \leq r_{max}$  and  $0 \leq \gamma \leq 2\pi$ .

### 1.1 Injection model of UPFC

To obtain an injection model for UPFC, it is first necessary to consider the series voltage source, Figure 3.

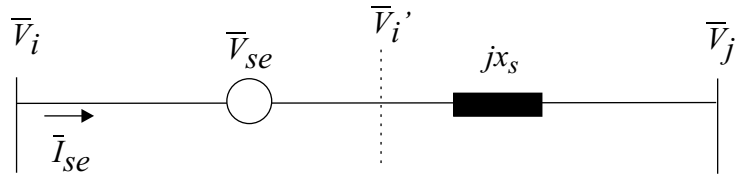


Figure 3: Representation of the series connected voltage source

The injection model is obtained by replacing the voltage source  $\bar{V}_{se}$  by a current source  $\bar{I}_{inj} = -jb_s\bar{V}_{se}$  in parallel with  $x_s$ , Figure 3.

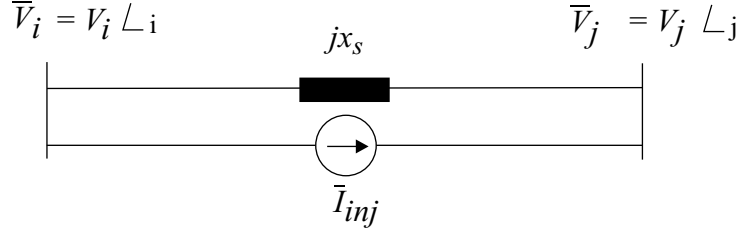


Figure 4: Transformed series voltage source

The current source  $\bar{I}_{inj}$  corresponds to injection powers  $\bar{S}_i$  and  $\bar{S}_j$  which are defined by

$$\bar{S}_i = \bar{V}_i (-\bar{I}_{inj})^* = -rb_s V_i^2 \sin(\gamma) - jrb_s V_i^2 \cos(\gamma) \quad (2)$$

$$\bar{S}_j = \bar{V}_j (\bar{I}_{inj})^* = rb_s V_i V_j \sin(\theta_{ij} - \gamma) + jrb_s V_i V_j \cos(\theta_{ij} - \gamma) \quad (3)$$

where  $\theta_{ij} = \theta_i - \theta_j$  and  $b_s = 1/x_s$ .

Figure 5 shows the injection model of the series part of UPFC, where

$$P_i = -\text{real}(\bar{S}_i), \quad Q_i = -\text{imag}(\bar{S}_i) \quad (4)$$

$$P_j = -\text{real}(\bar{S}_j), \quad Q_j = -\text{imag}(\bar{S}_j) \quad (5)$$

Having the UPFC losses neglected,

$$P_{CONV1} = P_{CONV2} \quad (6)$$

The apparent power supplied by the series voltage source converter is calculated from:

$$\bar{S}_{CONV2} = \bar{V}_{se} \bar{I}_{se}^* = re^{j\gamma} \bar{V}_i \left( \frac{\bar{V}_i' - \bar{V}_j}{jx_s} \right)^* \quad (7)$$

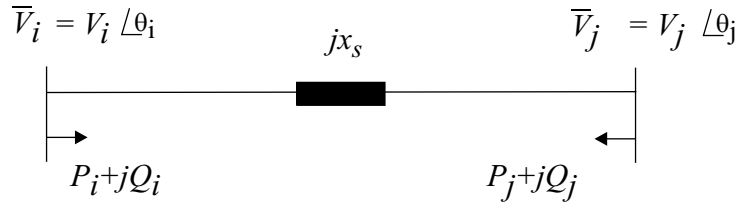


Figure 5: Injection model of the series part of the UPFC

Active and reactive power supplied by Converter 2 are distinguished as:

$$P_{CONV2} = rb_s V_i V_j \sin(\theta_i - \theta_j + \gamma) - rb_s V_i^2 \sin \gamma \quad (8)$$

$$Q_{CONV2} = -rb_s V_i V_j \cos(\theta_i - \theta_j + \gamma) + rb_s V_i^2 \cos \gamma + r^2 b_s V_i^2 \quad (9)$$

Afterwards, the series voltage source is coupled with the shunt part of the UPFC, which can be modeled as a separate controllable shunt reactive source. Here it is assumed that  $Q_{CONV1} = 0$ , but to allow for  $Q_{CONV1} \neq 0$  in the model is straight forward. Consequently, the UPFC injection model is constructed from series connected voltage source model with the addition of power equivalent to  $P_{CONV1} + j0$  to node  $i$ . The UPFC injection model is shown in Figure 6.

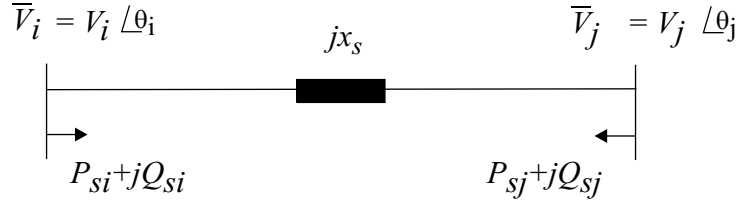


Figure 6: Injection model of the UPFC

In Figure 6

$$P_{si} = rb_s V_i V_j \sin(\theta_i - \theta_j + \gamma) \quad (10)$$

$$Q_{si} = rb_s V_i^2 \cos \gamma \quad (11)$$

$$P_{sj} = -P_{si} \quad (12)$$

$$Q_{sj} = -rb_s V_i V_j \cos(\theta_i - \theta_j + \gamma) \quad (13)$$

where  $r$  and  $\gamma$  are the control variables of the UPFC.

Besides the bus power injections, it is useful to have expressions for power flows from both sides of the UPFC injection model defined. At the UPFC shunt side, the active and reactive power flows are given as

$$P_{i1} = -rb_s V_i V_j \sin(\theta_{ij} + \gamma) - b_s V_i V_j \sin \theta_{ij} \quad (14)$$

$$Q_{i1} = -rb_s V_i^2 \cos \gamma + Q_{conv1} - b_s V_i^2 + b_s V_i V_j \cos \theta_{ij} \quad (15)$$

whereas at the series side they are

$$P_{j2} = rb_s V_i V_j \sin(\theta_{ij} + \gamma) + b_s V_i V_j \sin \theta_{ij} \quad (16)$$

$$Q_{j2} = rb_s V_i V_j \cos(\theta_{ij} + \gamma) - b_s V_j^2 + b_s V_i V_j \cos \theta_{ij} \quad (17)$$

The UPFC injection model is thereby defined by the constant series branch susceptance,  $b_s$ , which is included in the system bus admittance matrix, and the bus power injections  $P_{si}$ ,  $Q_{si}$ ,  $P_{sj}$  and  $Q_{sj}$ . If there is a control objective to be achieved, the bus power injections are modified through changes of the UPFC parameters  $r$ ,  $\gamma$ , and  $Q_{conv1}$ .

## 2 Rating of the UPFC

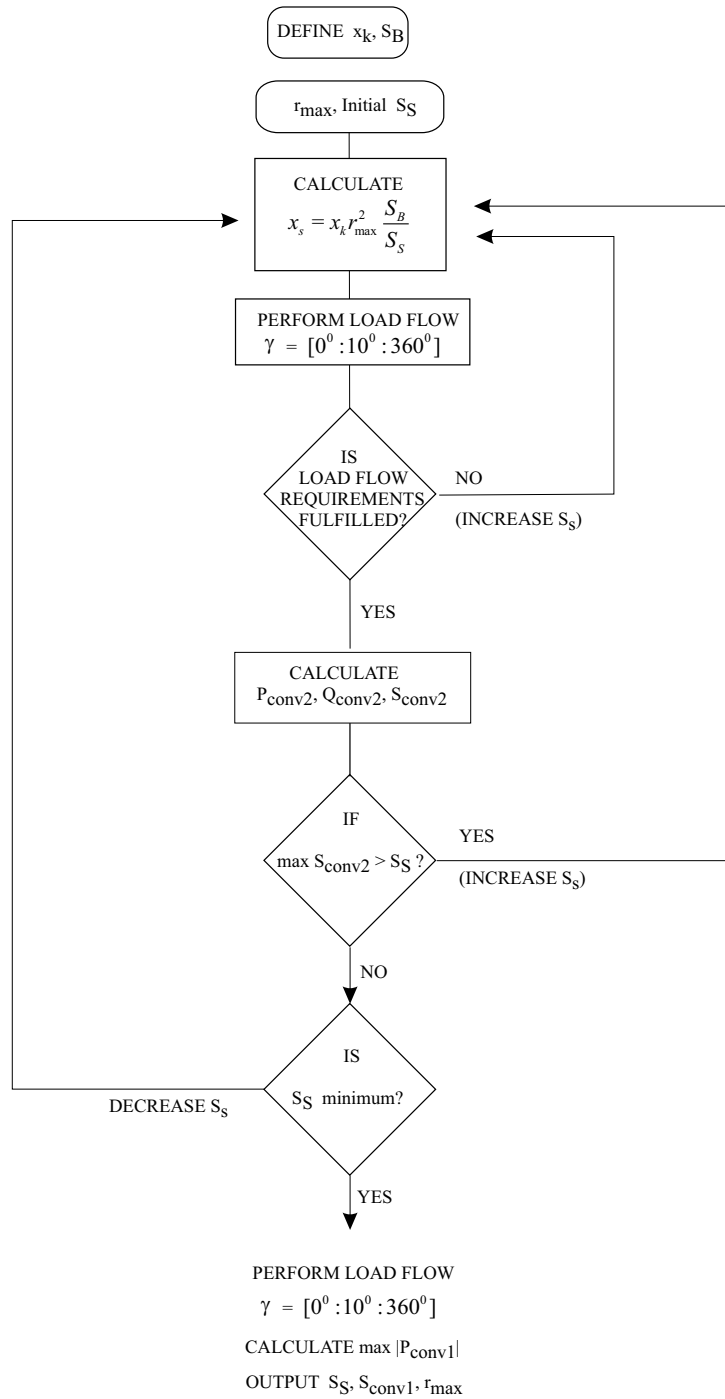


Figure 7: Algorithm for optimal rating of the UPFC

Operation of the UPFC demands proper power rating of the series and shunt branches. The rating should enable the UPFC carrying out pre-defined power flow objective. The flow chart of Figure 7 shows algorithm for UPFC rating.

The algorithm starts with definition of the series transformer short circuit reactance,  $x_k$ , and the system base power,  $S_B$ . Then, the initial estimation is given for the series converter rating power,  $S_S$ , and the maximum magnitude of the injected series voltage,  $r_{max}$ . The effective reactance of the UPFC seen from the terminals of the series transformer,  $(x_S)$ , can be determined in the next step.

Load flows are computed changing the angle  $\gamma$  between  $0^0$  and  $360^0$  in steps of  $10^0$ , with the magnitude  $r$  kept at its maximum value  $r_{max}$ . Such rotational change of the UPFC parameter influences active and reactive power flows in the system. The largest impact is given to the power flowing through the line with UPFC installed. Therefore, the regulation of the active and reactive power flow through the series branch of the UPFC could be set as initial pre-defined objective to be achieved within the UPFC steady state operation. Then, the load flow procedure is performed to check whether the pre-defined objective is achieved with satisfactory estimated parameters. If the load flow requirements are not satisfied at any operating points, it is necessary to go back in the algorithm, estimate again  $S_S$  and  $r_{max}$ , and perform new rotational change of the UPFC within the load flow procedure. This loop is performed until the load flow requirements are completely fulfilled. In addition, the active, reactive and apparent power of the series converter are calculated for each step change in the angle  $\gamma$ .

With the load flow requirements fulfilled and the series converter powers calculated, it has to be checked whether the maximum value of the series converter apparent power  $\max S_{conv2}$ , is larger than initially estimated power  $S_s$ . If  $\max S_{conv2}$  is not larger than the power  $S_S$ , it is necessary to check whether the power  $S_S$  is at an acceptable minimum level. If not, the value of  $S_S$  is reduced and the loop starts again. The acceptable minimum is achieved when two consecutive iterations do not differ more than the pre-established tolerance.

When the power  $S_S$  is minimized, the load flow procedure is performed with smaller step of rotational change of the angle  $\gamma(1^0)$ , in order to get maximum absolute value of the series/shunt converter active power,  $\max |P_{conv1}|$ . The value given by  $\max |P_{conv1}|$  is considered to be minimum criterion for dimensioning shunt converter rating power, whereas the power  $S_S$  represents series converter rating power as a function of the maximum magnitude  $r_{max}$ .

### 3 Power flow with the UPFC

The performance of the UPFC injection model is tested on the two area four generator power system shown in Figure 8. The 230 km interconnecting tie line carries 400MW from area 1 (generators 1 and 2) to area 2 (generators 3 and 4) during normal operating conditions. The injection model of the UPFC is placed at the beginning of the lower line between buses 8 and 12 in order to see the influence on the power flow through that line as well as on the bus voltages. According to the algorithm for rating of the UPFC,  $r_{max}$ ,

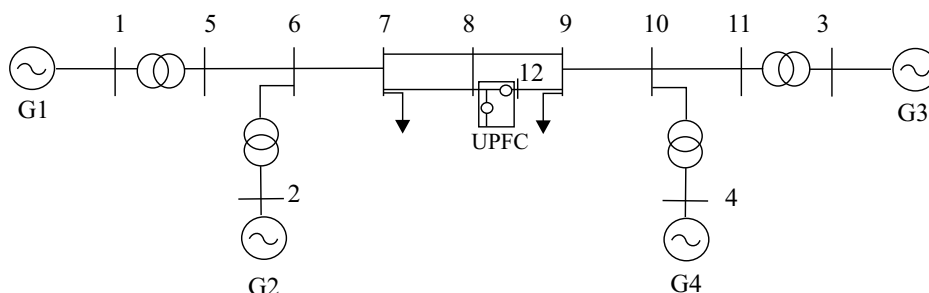


Figure 8: Two area system with the UPFC installed

$S_S$  and  $\max|P_{conv1}|$  are defined, although  $\max|P_{conv1}|$  basically is not needed in this test because the shunt part is inactive. For the value of  $r_{max} = 0.15$  pu, the corresponding powers  $S_S$  and  $\max|P_{conv1}|$  are equal to 0.40 pu, and 0.2737 pu, respectively. That value of  $r_{max}$  is usually estimated to be acceptable for voltage/power flow control purposes, [2].

Having the UPFC shunt part inactive ( $I_{conv1} = 0$ ), the UPFC has two control parameters,  $r$  and  $\gamma$ , the magnitude and the phase of the injected voltage respectively. Thereby, the shunt side voltage  $V_i$  cannot be controlled.

Figures 9, 10, and 11 show active power flow in line 8, where the UPFC is located. Figure 9 shows the power flow in line 8 where  $\gamma$  is kept constant at various values while  $r$  varies from 0 to 0.15. It can be seen that the controllability of the power flow with  $r$  is maximal when  $\gamma = \pi/2$  for increasing power flow and when  $\gamma = 3\pi/2$  for decreasing load flow. The relationship between  $r$  and active power flow is monotonic for fixed  $\gamma$ .

Figure 10 shows the same active power flow in line 8 but with respect to rotational change in  $r$  and  $\gamma$ . That means,  $r$  is kept constant at some values for a full circle of the angle  $\gamma(0^0 : 360^0)$ . Is it obvious that the active power flow is maximal when  $r$  is maximal. The active power flow in the system without UPFC in line 8, is  $P_{base} = 1.9526$ , whereas the maximum change in positive directions equal to +0.6012 pu, and in negative direction  $-0.6711$  pu. It means that by inserting the maximum value of the magnitude  $r(0.15pu)$ , the

active power in line 8, could be changed by maximum 54.47 MW in positive direction or by 48.98 MW in negative one, if the angle  $\gamma$  is appropriately adjusted. The maximum active power flow conditions occur around  $70^\circ$  and  $250^\circ$ . Figure 11 shows the relations of the both parameters in single three dimension picture.

Figures 12 and 13 show the bus voltages at the series and shunt side of UPFC, with respect to the rotational change in  $r$  and  $\gamma$ . Because the third parameter of the UPFC,  $Q_{conv1}$ , is inactive,  $V_i$  is not controlled in this case. As can be seen the voltage magnitude have opposite directions. One of them has magnitude increased when the other one is decreased.

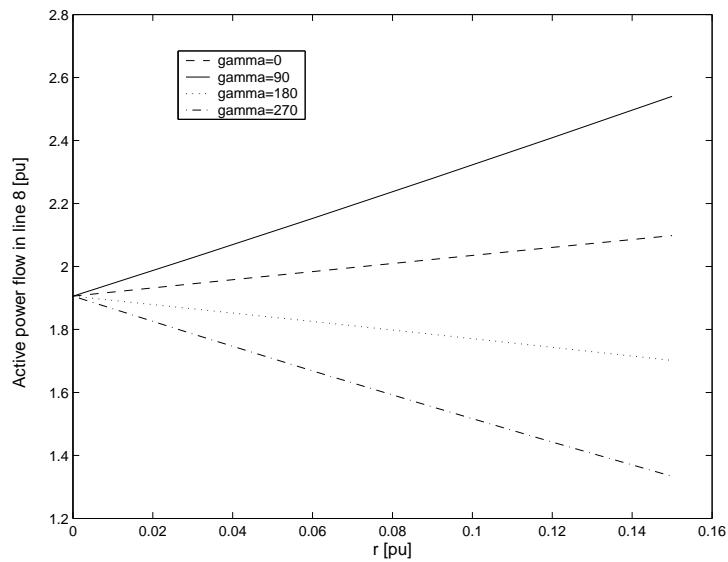


Figure 9: Active power flow in line with UPFC;  $\gamma = const.$



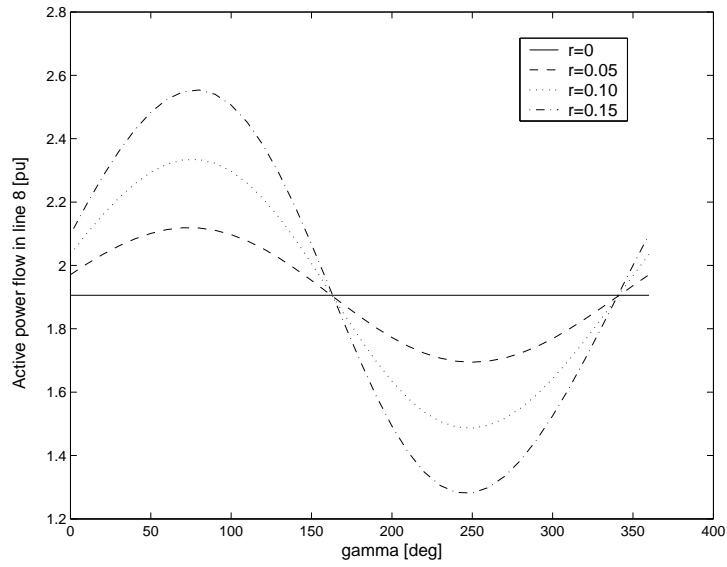


Figure 10: Active power flow in line with UPFC;  $r = const.$

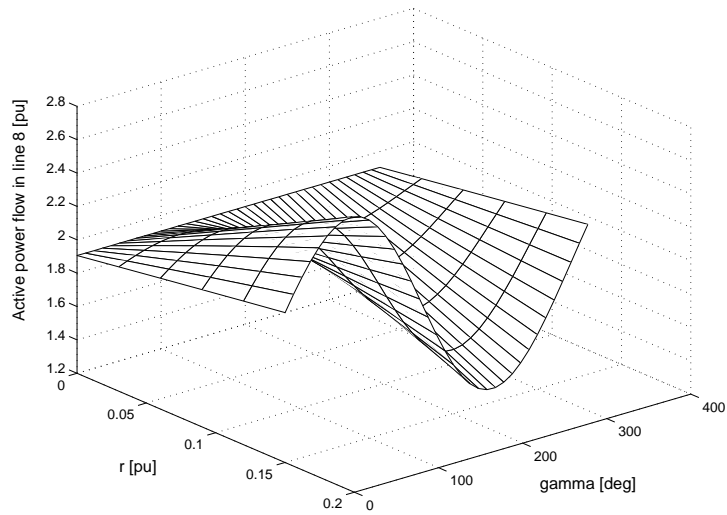


Figure 11: Active power flow in line with UPFC

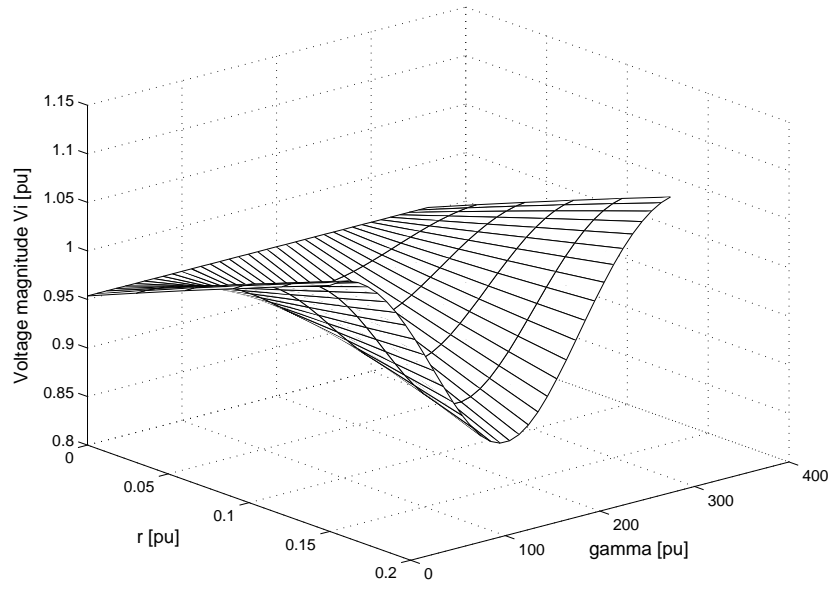


Figure 12: Series side bus voltage magnitude  $V_i = f(r, \gamma)$

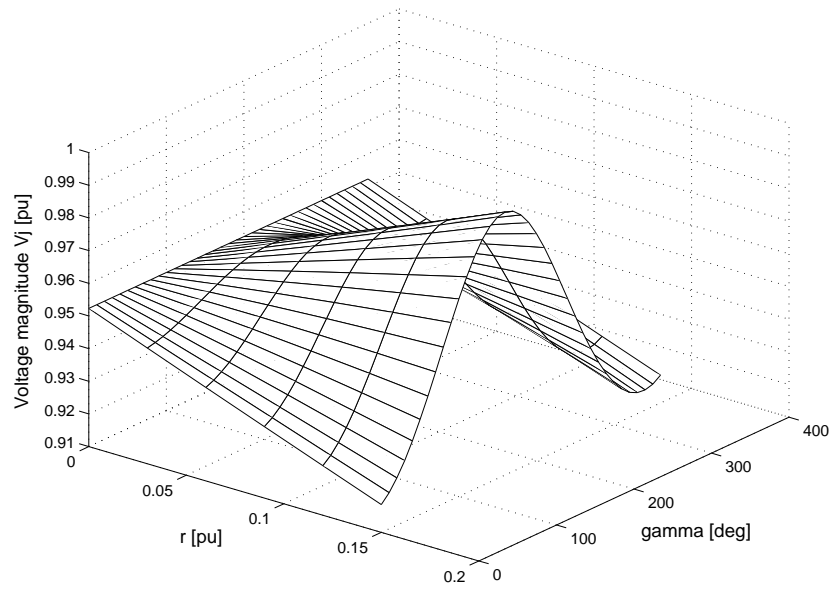


Figure 13: Shunt side bus voltage magnitude  $V_j = f(r, \gamma)$

## 4 System models

### 4.1 Synchronous machine model

Mathematical models of a synchronous machine vary from very elementary classical models to more detailed ones. In the detailed models, transient and subtransient phenomena are considered. Here, the transient models are used to represent the machines in the system, according to following equations.

**Stator winding equations:**

$$v_q = -r_s i_q - x_d' i_d + E_q' \quad (18)$$

$$v_d = -r_s i_d + x_q' i_q + E_d' \quad (19)$$

where

$r_s$  is the stator winding resistance

$x_d'$  is the  $d$ -axis transient resistance

$x_q'$  is the  $q$ -axis transient resistance

$E_q'$  is the  $q$ -axis transient voltage

$E_d'$  is the  $d$ -axis transient voltage

**Rotor winding equations:**

$$T_{do}' \frac{dE_q'}{dt} + E_q' = E_f - (x_d - x_d') i_d \quad (20)$$

$$T_{qo}' \frac{dE_d'}{dt} + E_d' = (x_q - x_q') i_q \quad (21)$$

where

$T_{do}'$  is the  $d$ -axis open circuit transient time constant

$T_{qo}'$  is the  $q$ -axis open circuit transient time constant

$E_f$  is the field voltage

**Torque equation:**

$$T_{el} = E_q' i_q + E_d' i_d + (x_q' - x_d') i_d i_q \quad (22)$$

**Rotor equation:**

$$2H \frac{d\omega}{dt} = T_{mech} - T_{el} - T_{damp} \quad (23)$$

$$T_{damp} = D\Delta\omega \quad (24)$$

where

$T_{mech}$  is the mechanical torque, which is constant in this model

$T_{el}$  is the electrical torque

$T_{damp}$  is the damping torque

$D$  is the damping coefficient.

The  $d$  and  $q$ -axis block diagrams of the stator fluxes for the transient model is presented in Figure 14, and the block diagram for computation of torque and speed in the transient generator model is presented in Figure 15.

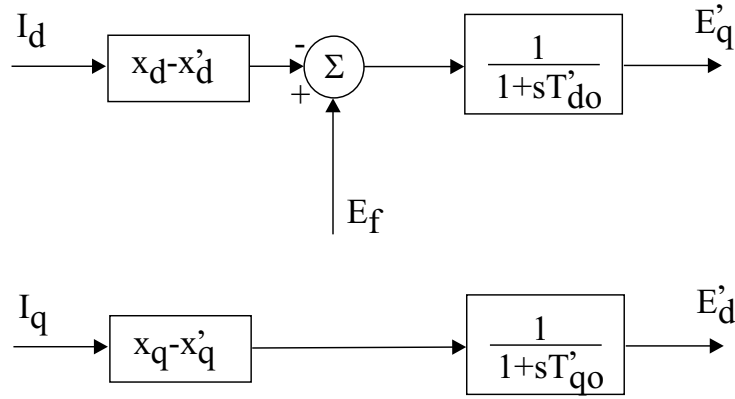


Figure 14: Block diagram for the transient generator model

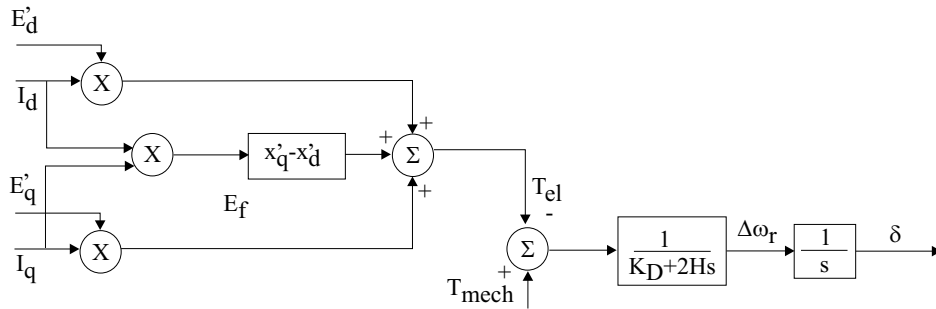


Figure 15: Block diagram for computation of torque and speed in the transient generator model

For time domain simulation studies, it is necessary to include the effects of the excitation controller. Automatic voltage regulators (AVRs) define the primary voltage regulation of synchronous machines [3]. AVR and exciter model for synchronous generator is modeled as the standard IEEE model, Figure 16.

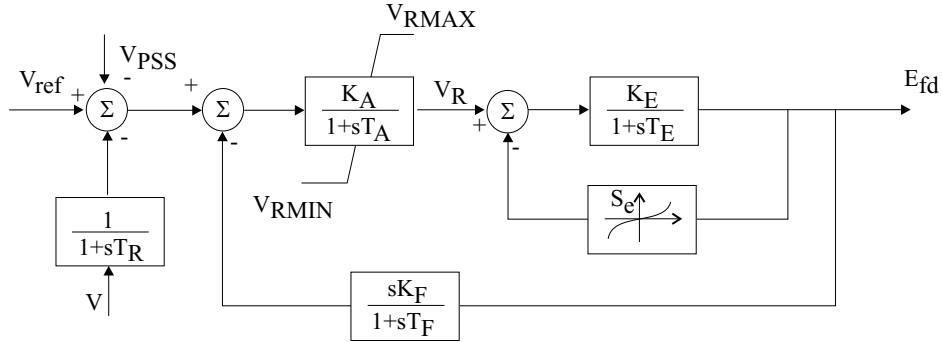


Figure 16: AVR and exciter model for synchronous generator

## 4.2 Load model

The loads can be modeled using constant impedance, constant current and constant power static load models [3]. Thus,

1. Constant impedance load model (constant Z): A static load model where the real and reactive power is proportional to the square of the voltage magnitude.
2. Constant current load model (constant I): A static load model where the real and reactive power is directly proportional to the voltage magnitude.
3. Constant power load model (constant PQ): A static load model where the real and reactive powers have no relation to the voltage magnitude.

All these load models can be described by the following equations:

$$P = P_0 \left( \frac{V}{V_0} \right)^\alpha$$

$$Q = Q_0 \left( \frac{V}{V_0} \right)^\beta$$

where  $P_0$  and  $Q_0$  stand for the real and reactive powers consumed at a reference voltage  $V_0$ . The exponents  $\alpha$  and  $\beta$  depend on the type of the load that is being represented; for constant power load models  $\alpha = \beta = 0$ , for constant current load models  $\alpha = \beta = 1$  and for constant impedance load models  $\alpha = \beta = 2$ .

### 4.3 Power system stabilizer model

A PSS can be viewed as an additional control block used to enhance the system damping. This block is added to AVR.

The three basic blocks of a typical PSS model, are illustrated in Figure 17. The first block is the stabilizer Gain block, which determines the amount of damping. The second is the Washout block, which serves as a high-pass filter, with a time constant that allows the signal associated with oscillations in rotor speed to pass unchanged, but does not allow the steady state changes to modify the terminal voltages. The last one is the phase-compensation block, which provides the desired phase-lead characteristic to compensate for the phase lag between the AVR input and the generator torque.

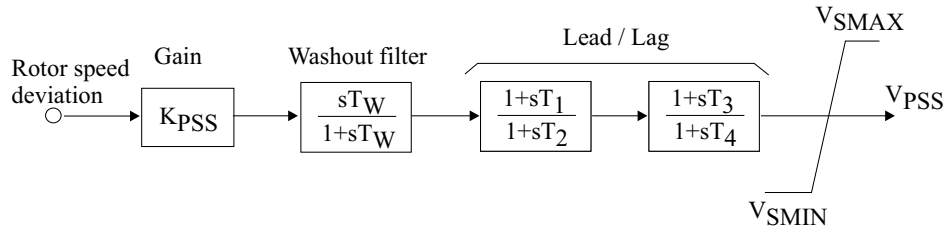


Figure 17: PSS block diagram

### 4.4 UPFC

Injection model of the UPFC is described in the static part of the analysis, where the power injection model is used. However, for a dynamic analysis, due to model requirements, current injection model is more appropriate. Figure 18 which illustrates the UPFC electric circuit arrangement is repeated here due to clarity. In Figure 18,

$$\bar{I}_{sh} = \bar{I}_t + \bar{I}_q = (I_t + j * I_q)e^{j\theta_i} \quad (25)$$

where  $\bar{I}_t$  is the current in phase with  $\bar{V}_i$  and  $\bar{I}_q$  is the current in quadrature with  $\bar{V}_i$ . In Figure 19 the voltage source  $\bar{V}_{se}$  is replaced by the current source  $\bar{I}_{inj}$ .

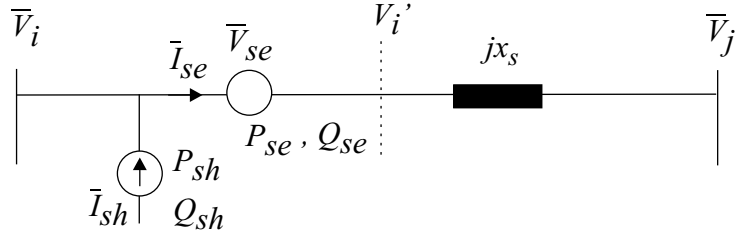


Figure 18: The UPFC electric circuit arrangement

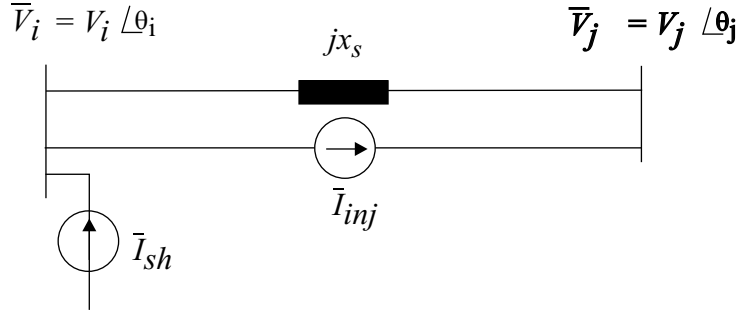


Figure 19: Transformed series voltage source

The active power supplied by the shunt current source can be calculated from

$$P_{CONV1} = \text{Re}[\bar{V}_i(-\bar{I}_{sh})^*] = -V_i I_t \quad (26)$$

From the static part we have equations:

$$P_{CONV1} = P_{CONV2} \quad (27)$$

$$P_{CONV2} = r b_s V_i V_j \sin(\theta_i - \theta_j + \gamma) - r b_s V_i^2 \sin \gamma \quad (28)$$

From last three equations we have

$$I_t = -r b_s V_j \sin(\theta_i - \theta_j + \gamma) + r b_s V_i \sin \gamma \quad (29)$$

The shunt current source is calculated from

$$\bar{I}_{sh} = (I_t + j * I_q) e^{j\theta_i} = (-r b_s V_j \sin(\theta_{ij} + \gamma) + r b_s V_i \sin \gamma + j I_q) e^{j\theta_i} \quad (30)$$

From the Figure 19 can be defined,

$$\bar{I}_{si} = \bar{I}_{sh} - \bar{I}_{inj} \quad (31)$$

$$\bar{I}_{sj} = \bar{I}_{inj} \quad (32)$$

where, from the static part,

$$\bar{I}_{inj} = -jb_s \bar{V}_{se} = -jb_s r \bar{V}_i e^{j\gamma} \quad (33)$$

Inserting Equations 30 and 33 into Equations 31 and 32 yields

$$\bar{I}_{si} = (-rb_s V_j \sin(\theta_{ij} + \gamma) + rb_s V_i \sin \gamma + jI_q) e^{j\theta_i} + jrb_s V_i e^{j(\theta_i + \gamma)} \quad (34)$$

$$\bar{I}_{sj} = -jrb_s V_i e^{j(\theta_i + \gamma)} \quad (35)$$

where  $I_q$  is independently controlled variable, like a shunt reactive source from the power injection model of UPFC. Based on previous Equations, current injection model can be presented as in Figure 20.

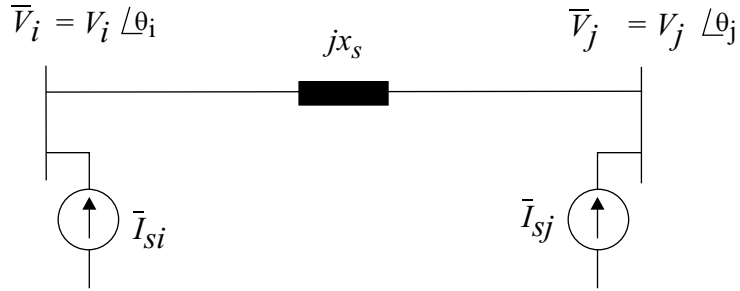


Figure 20: The UPFC current injection model

## 4.5 Results

The two area system is shown again here, due to clarity in Figure 21. The system data can be found in [3]. The system model is used as it is described above, but without PSS. The active and reactive components of loads have constant current characteristics ( $\alpha = \beta = 1$ ).

The UPFC is installed in line 8, according to Figure 21. Suppose that the fault occurs in the system at point F. The fault is cleared after 100 ms by opening the faulted line. Figure 22 illustrates the active power flow in line 8 in that case, for the system with and without the UPFC. The UPFC is not controlled. The parameters of the UPFC are chosen based on static behavior



of the UPFC. This test case is made to verify the current injection model of the UPFC. With the control of the variables  $r$  and  $\gamma$ , improvements in damping of the oscillations should be obvious.

Figure 23 proposes the general form of the UPFC control system. The UPFC should operate in the automatic power flow control mode keeping the active and reactive line power flow at the specified values. This can be achieved by the linearizing the line power flow equations 16 and 17 around the starting point resulting in the gain matrix in Figure 23.  $\Delta\gamma$  and  $\Delta r$  are the changes in the control variables, assuming that the third control variable  $I_q$  is inactive. Figures 24 and 25 show the first preliminary results of the proposed control method if the specified value of the active power is  $P_{sp} = 2.5[pu]$  and the reactive power,  $Q_{sp} = -0.02[pu]$ , see Figures 24 and 25. The starting point is defined at  $P_{base} = 2.1526[pu]$  and  $Q_{base} = -0.1798[pu]$ . An alternative control strategy for the UPFC to be investigated is based on the series voltage  $u_{dq}$  injected by the UPFC.

If  $u_{dq}$  is the instantaneous voltage injected by the UPFC, the components  $u_d$  and  $u_q$  can be related to the control variables

$$u_d = r \cos(\gamma) \quad , \quad u_q = r \sin(\gamma) \quad (36)$$

and hence

$$r = \sqrt{u_d^2 + u_q^2} \quad , \quad \gamma = \arctan\left(\frac{u_q}{u_d}\right) \quad (37)$$

The further studies will investigate these two control methods with respect to performance and robustness.

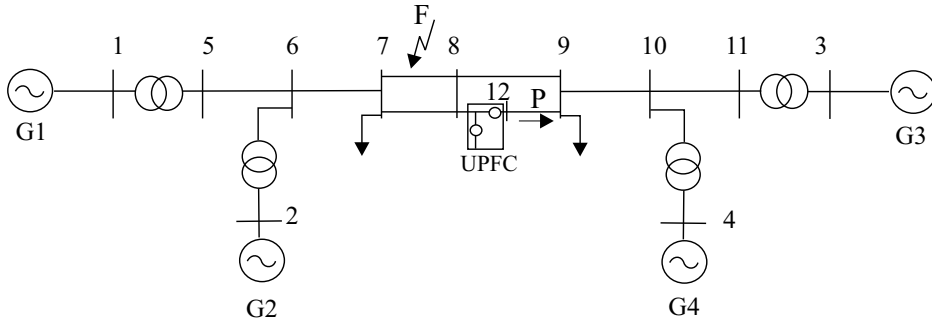


Figure 21: The two area system with UPFC installed in line 8

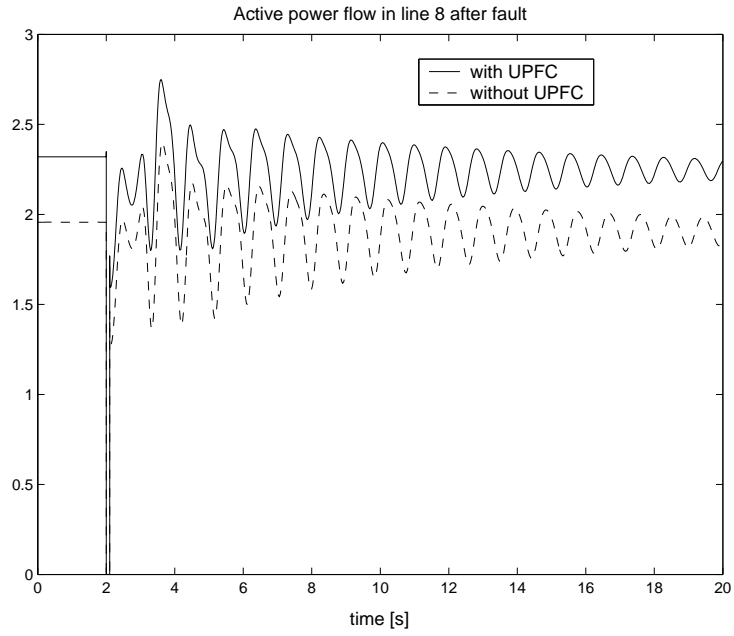


Figure 22: The active power flow in the line 8 with UPFC installed after fault applied

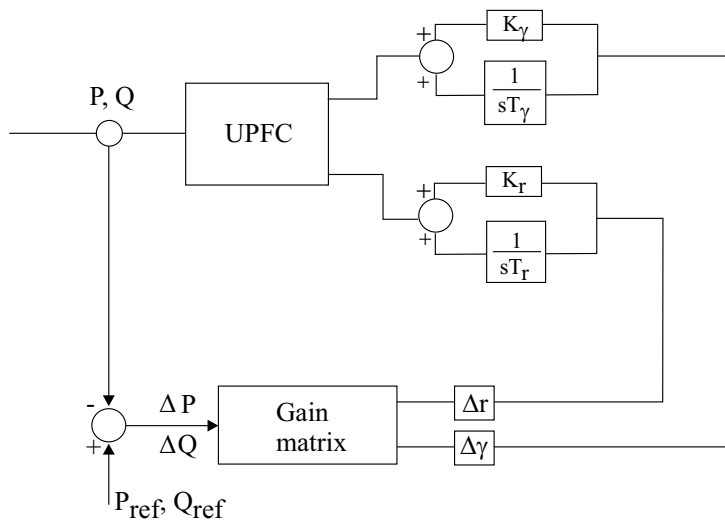


Figure 23: General form of the UPFC control system

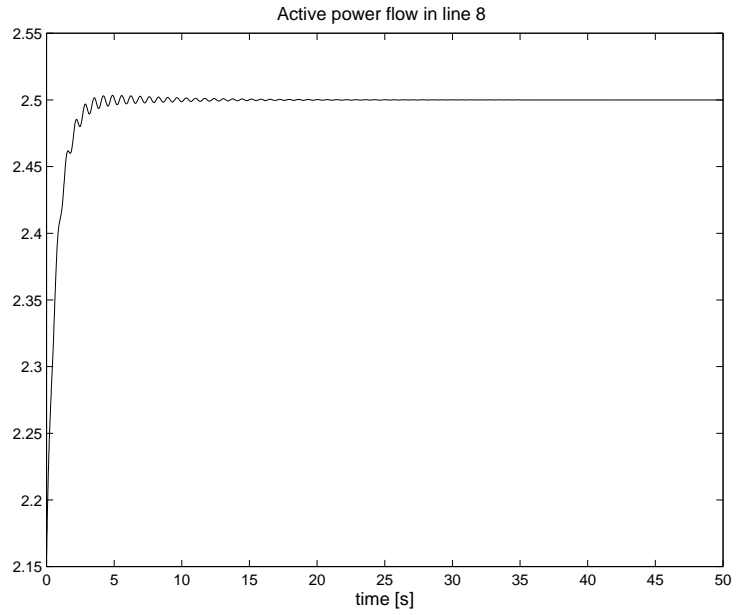


Figure 24: Controlled active power flow

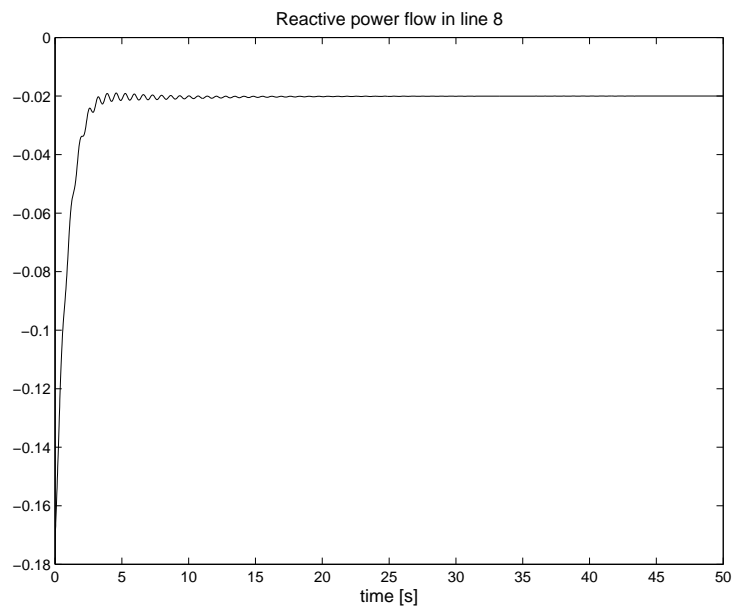


Figure 25: Controlled reactive power flow

## 4.6 Appendix

The generator parameters in per unit are as follows:

$$\begin{aligned} X_d &= 1.8 & X_q &= 1.7 & X'_d &= 0.3 & X'_q &= 0.55 & R_a &= 0.0025 \\ X_l &= 0.2 & T'_{d0} &= 8s & T'_{q0} &= 0.4s & H &= 6.5 \text{ (for G1 and G2)} \\ H &= 6.175 \text{ (for G3 and G4)} & D_w &= 0 \end{aligned}$$

The exciter parameters in per unit are as follows:

$$\begin{aligned} K_A &= 20 & T_A &= 0.055 & T_E &= 0.36 & K_E &= 0 & K_F &= 0.125 \\ T_F &= 1.8 & A_{ex} &= 0.0056 & B_{ex} &= 1.075 & T_R &= 0.05 \end{aligned}$$

The UPFC parameters in per unit are as follows:

$$\begin{aligned} r_{max} &= 0.09 & \gamma &= 90^0 & S_s &= 0.4 & I_q &= 0 & K_\gamma &= 2 \\ T_\gamma &= 0.2 & K_r &= 0.02 & T_r &= 0.02 \end{aligned}$$

## 4.7 References

- [1] R. Sadikovic, Single-machine infinite bus system, internal report, July 2003
- [2] N. Dizdarevic, Unified Power Flow Controller in Alleviation of Voltage Stability Problem , Doctoral thesis, Zagreb, 2001
- [3] P. Kundur, Power System Stability and Control, McGraw-Hill, Inc.,1993
- [4] Z.J. Meng, P.L.So, A Current Injection UPFC Model for Enhancing Power System Dynamic Performance
- [5] Power System Toolbox, Version 2.0, Cherry Tree Scientific Software, Ontario, Canada